5

GRB030329: A Complicated Evolution

GRB030329 afterglow, due to its proximity, allowed an extensive coverage in all wavebands. The rich data set in optical, radio and millimeter bands [85, 111] along with polarisation lightcurves [61] and size measurements of the fireball [131], made unprecedented follow up in the history of afterglow research. Rewarding all these efforts, the afterglow revealed novel features. The optical lightcurve initially followed the usual behaviour of a power-law decay, with an achromatic steepening around half a day. It started deviating from this simple and familiar model around ~ 1.5 days, displaying a sharp jump of ~ 0.5 mag and substantial variability. At radio frequencies, the behaviour was puzzling. The flux evolved much slower than expected from a model appropriate to the optical evolution. Steepening of the radio lightcurves were observed at ~ 10 days instead of 0.5 days after the burst [11]. In addition, the optical light curve also had a significant contribution from the underlying supernova SN2003dh after about a week following the burst.

In order to explain this complicated evolution, Berger et al. [11] introduced a double-jet model, with a narrow jet responsible for the early optical emission and a wider jet contributing to the radio and late-time optical and X-ray emission. The sharp bump in the optical light curve seen at ~ 1.5 days has been attributed to the deceleration epoch of the wider jet [11].

Granot et al. [59] have instead proposed that the bump in the R-band lightcurve at 1.5 days and at three successive epochs could be attributed to refreshed shocks. In their original model, however, the second jet break at $\sim$ 10 days was not expected

In this chapter, we examine the ability of the double jet model to fit the multi-band observations of the afterglow. We present a refined set of parameters for the two jets resulting from our fits. We also examine whether the two jets are in fact distinct entities or whether a refreshed shock might have converted the decelerating narrow jet to a wider, more energetic jet.

5.1 The Model

The basic quantity in our model is the synchrotron source function, which we consider to have appropriate power-law forms between the usual break frequencies. Transition from one power-law phase to another is made gradual through a Band type smoothening [5] at the peak frequency ν_m and the cooling frequency ν_c. The self-absorption frequency ν_a is not treated as a break; instead the absorption is incorporated into the expression for synchrotron optical depth, which, along with the source function, yields the flux at any given frequency. In the co-moving frame of the shock, the optical depth is set to unity at $\nu = \nu_a$(comoving). We incorporate transition to the non-relativistic phase, as in Frail et al. [50]. The non-relativistic transition is treated as a sharp break at a time $t = t_{\rm nr}$. We obtain our fits through the usual χ^2 minimization procedure, using $\nu_a, \nu_m, \nu_c, t_{\rm nr}$, the electron distribution index p and the jet break time t_j as the fit parameters. Here we are trying to model the underlying smooth power law behaviour rather than the short time scale variabilities in the lightcurve. Since our model does not include the short-term variabilities, the nominal χ^2 obtained is relatively high. The best fit from this model is shown in figures 5.1 – 5.4 We derived the physical parameters $\mathcal{E}_{\rm iso}$, ϵ_e and ϵ_B using the expressions in Wijers & Galama [142] from these fitted parameters, with appropriate modifications to place ν_a at $\tau_\nu = 1$ instead of 0.35 used by Wijers & Galama.

5.2 The double jet model for GRB030329

The X-ray and optical lightcurves of GRB030329 afterglow had an initial temporal slope of ~ -0.9. Around half a day, the optical decay steepened to an index of ~ -1.9. Sampling of the X-ray evolution was poor, but an interpolation of the *RXTE* and *XMM* data obtained during ~ 0.1 to ~ 100 days indicated a break almost at the same time as the optical steepening mentioned above [132]. A nearly simultaneous break observed in frequencies separated by four orders of magnitude suggested that the break observed at ~ 0.5 days was a jet break.

At radio frequencies, the first observations obtained were around 1 days, somewhat later than the epoch of the jet break obtained from optical and X-ray observations. The radio and millimeter light curves, however, did not display the behaviour expected after a jet break at 0.5 days. Instead, they were rather well described by a second jet, with a jet break around 10 days [11, 123]. The optical light curve showed a re-brightening around 1.5 days, followed by a slower decay consistent with that expected from the second jet to which the radio emission was attributed [11, 85]. The optical re-brightening at 1.5 days was attributed to the epoch of deceleration of the second jet. Berger et al. [11] estimated the initial opening angle of the first (narrow) jet to be $\sim 5^\circ$ and that of the second (wide) jet to be $\sim 18.4^\circ$. The energy contents of the two jets were estimated to be $\sim 6.7 \times 10^{48}$ erg for the narrow jet and $\sim 10^{50}$ erg for the wide jet. Compared to the narrow jet, a later deceleration epoch implied a smaller initial Lorentz factor for the wide jet, and correspondingly a much higher initial baryon load. The double jet model has been found to be consistent with most observations reported till date. The optical emission at late times ($t > 10$ days) is, however, dominated by the associated supernova SN2003dh.

We attempted modeling the multiband observations within the ambit of this double-jet model (model 1).

5.2.1 The wide jet

The parameters of the wide jet are well constrained by data in the 4–250 GHz range [11, 123]. At the jet break time of 9.8 days, we find the self absorption

frequency ν_a to be $1.3^{+0.25}_{-0.06} \times 10^{10}$ Hz, the synchrotron peak frequency ν_m to be $3.98^{+0.5}_{-0.1} \times 10^{10}$ Hz with a peak flux f_{ν_m} of $44.7^{+1.0}_{-2.0}$ mJy. The post jet-break decay in radio, the peak optical flux at 1.5 days and the late X-ray observations at 37 and 61 days together constrain the electron energy distribution index p to $2.3^{+0.05}_{-0.02}$ and the cooling frequency ν_c to $3.98^{+1.3}_{-2.0} \times 10^{14}$ Hz after the jet break. These parameter values are very similar to those derived by Berger et al. [11]. The 1280 MHz observations from *GMRT* show a gradual rise of flux to a peak around 133 days. This behaviour can be reproduced by a non-relativistic transition of the jet at $t_{\rm nr} = 42^{+17}_{-7}$ days.

5.2.2 The narrow jet

The jet break time for the narrow jet is derived to be $0.69^{+0.08}_{-0.06}$ days from the optical light curve. Using a galactic extinction $E(B-V) = 0.025$ mag in the direction of the GRB [121], the early optical and X-ray observations, both before and after this break, are well described by an electron energy distribution index p of 2.12 ± 0.05. Some authors [85, 119] have conjectured that there occurs a passage of the cooling break (ν_c) through optical bands within the first few hours after the GRB, based on a derived change in slope of R-band light curve around $\sim$ 0.25 days, and a small color evolution. The observations from the Himalayan Chandra Telescope (HCT) and The Sampurnanand Telescope (ST) have a continuous coverage from $\sim$ 0.15 days to $\sim$ 0.3 days after the burst, taken from the same instrument and calibrated uniformly on the same scale. The data over this interval are fit very well by a single power law [111]. Even the data reported by Sato et al. [119] and Lipkin et al. [85] do not conclusively demonstrate a secular steepening at $\sim$ 0.25 days; the effect could be easily mimicked by short-term variability riding on a single, underlying power law. Gorosabel et al. [56], from their quasi-simultaneous multicolour lightcurves from 0.4 to 0.65 day do not derive any signature of the color evolution. Colors derived from multiband observations from HCT and ST have somewhat large errors ($\sim$ 0.08 mag 1-σ), and we are unable to discern the $\sim$ 0.1 mag systematic change in $B-R$ color reported [85]. As mentioned by Lipkin et al. [85], there could be various reasons for this early color evolution. We do not feel that the passage of cooling break

through optical bands at early times can be conclusively established from the existing observations. From multiband fits, however, we estimate ν_c to be at $1.0^{+1.0}_{-0.5} \times 10^{16}$ Hz at 0.5 days. At times > 1.5 days, the contribution from the wide jet is sufficient to reproduce the radio light curves (see figures 5.1– 5.4), so the radio emission from the narrow jet is constrained to be almost negligible. In order to achieve this, we need to have the peak frequency ν_m and the self absorption frequency ν_a of the narrow jet to be as high as possible. The passage of ν_m is not observed through the optical band, so we chose it to be just below the R-band at the earliest epoch (~ 0.05 days) at which data are available. This results in ν_m regressing to $\sim 10^{13}$ Hz at the jet break epoch of 0.5 days. The fitted peak flux $F_{(\nu=\nu_m)}$ is $19.8^{+9.3}_{-2.4}$ mJy at this time. The density of the ambient medium can be derived from the rather well-constrained parameters of the wide jet, and works out to be $n \sim 8$ atom/cc. This, along with the narrow jet parameters mentioned above, predicts the self absorption frequency of the narrow jet to be ν_a equal to $3.1^{+0.14}_{-0.63} \times 10^9$ Hz at 0.5 days. We find that this value of ν_a yields adequate suppression of the narrow jet flux at low frequencies for the model to be consistent with the GMRT data.

As mentioned earlier, the $\chi^2_{\rm DOF}$ is somewhat high due to short-term variabilities in the observed light curve. From the fit we excluded the first seven days of data at 4.86 and 8.46 GHz, which appear to have been affected by scintillations. The first data point at 250 GHz (~ 1.5 days) and at 100 GHz (0.8 days) were also removed from the fit. We did not consider five more data points in radio bands (of 2.6 days in 43 GHz, days 1 and 12 in 22 GHz and days 3.5 and 4.7 in 15 GHz) which produced high χ^2 values due to scatter. We excluded the optical data from discussion for epochs larger than ~ 5 days because of the dominant contribution from SN2003dh. A $\chi^2_{\rm DOF}$ of 23.3 is obtained for the best fit with this model. The optical (mostly V and B) bands dominate the contribution to χ^2 along with the lower radio frequencies (4 GHz, 8 GHz and 15 GHz). The number density of the ambient medium is inferred to be 8.6^{+12}_{-5}. We infer the fractional energy content in relativistic electrons and magnetic field to be $0.56^{+0.4}_{-0.5}$ and $4^{+1.9}_{-1.8} \times 10^{-4}$ respectively for the narrow jet, and $9.0^{+3}_{-1} \times 10^{-2}$ and $11.9^{+10}_{-7} \times 10^{-4}$ for the wide jet. We derive $4.3^{+1.3}_{-0.8} \times 10^{52}$ erg for the isotropic equivalent energy and $6.2^{+0.02}_{-0.03}$ degrees. for the opening angle of narrow jet. This corresponds to a total energy

content of $1.5^{+4.8}_{-2.4} \times 10^{50}$ erg in the jet. For the wide jet, we derive an isotopic equivalent energy of $5.4^{+0.4}_{-0.2} \times 10^{52}$ erg, opening angle of $18.7^{+0.07}_{-0.04}$ degrees. and a total energy of $4.9^{+3.3}_{-2.1} \times 10^{50}$ erg.

We calculated the rising flux from the wide jet at $t < 1.5$ days, assuming time evolution of the spectral parameters to be of the form $\nu_m \propto t^0$, $\nu_c \propto t^{-2}$, $f_{\nu_m} \propto t^3$ [101] and $\nu_a \propto t^1$ and normalizing them at 1.5 days.

We also explored the possibility of the ambient medium of the burst being generated by a stellar wind, with a density profile of $n(r) \propto r^{-2}$, but were unable to obtain consistent fits with the double-jet model. If the model is tuned to reproduce radio data in the 8–43 GHz frequency range, it leads to an overprediction of fluxes in millimeter bands and an underprediction at 1280 MHz.

5.3 Refreshed Jet ?

Most of the observations are well reproduced by a model which sums the contributions from the wide and narrow jet. However, the ability of the model to reproduce the sharpness of the 1.5 day kink has been questioned by ([101]). Moreover, we note that the contribution of the narrow jet is almost negligible at radio bands; in fact the wide jet alone is quite sufficient to account for the observed flux after ~ 1.5 days. It therefore appears to us that the data could be well described if, instead of both jets contributing simultaneously to the emission, the narrow jet alone contributes at epochs earlier than ~ 1.5 days, and only the wide jet after that time. This suggests that a possible re-energization event around or before ~ 1.5 days could have refreshed the initially narrow jet, which had entered the lateral expansion phase, and given it additional forward momentum, converting it into the second, 'wide' jet. The opening angle of the laterally expanding, initially narrow jet around ~ 1.5 days is estimated to be $\sim 20°$, not far from the initial opening angle inferred for the wide jet ($\sim 18°$). We therefore consider it possible that a re-energization event occurred after the jet break of the narrow jet [59] and the double-jet model for GRB030329 could represent the conversion of an initially narrow jet to a wide one by the re-energization.

In a simple representation of such a re-energization, we assume that the phys-

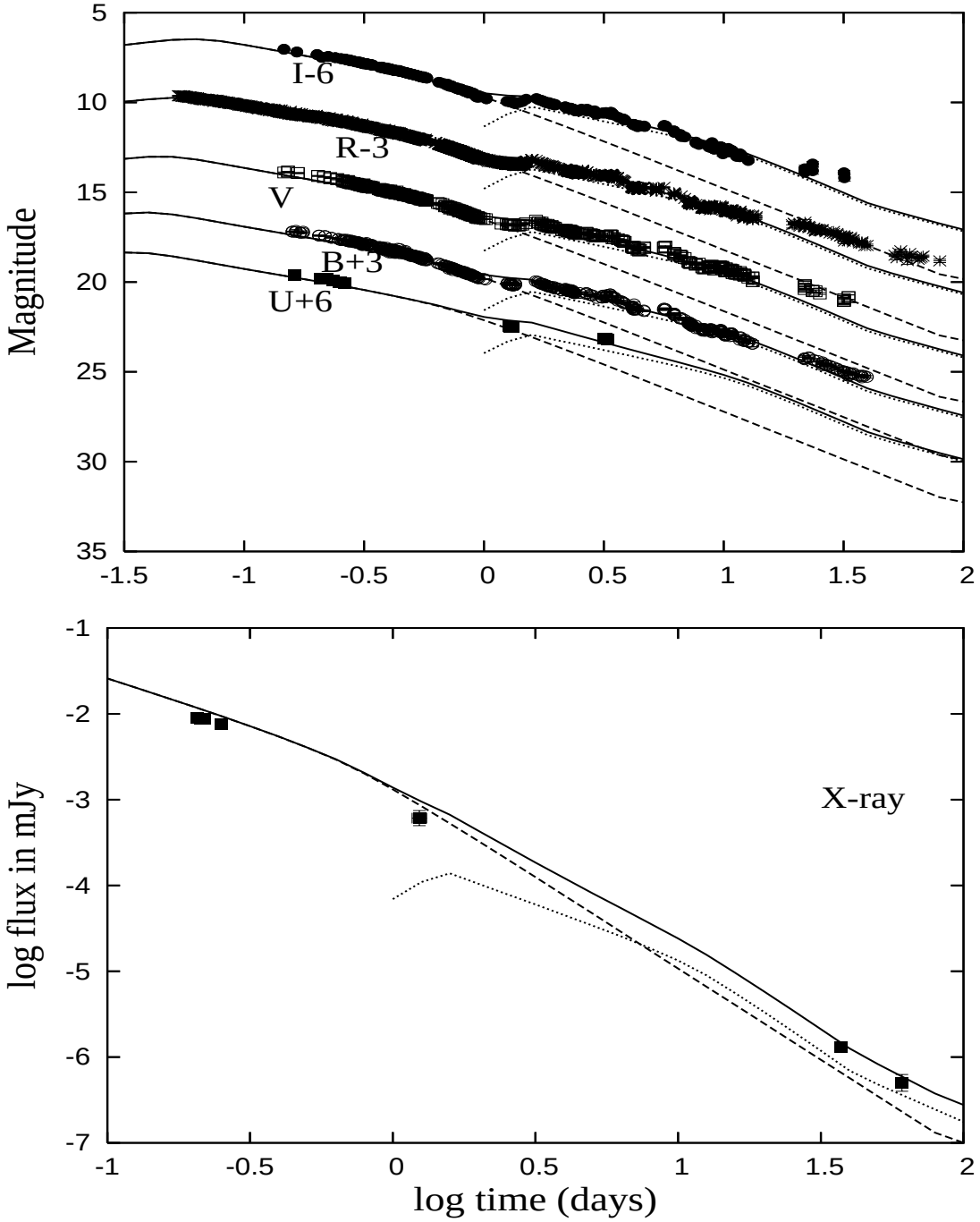

Figure 5.1. (top panel) The Optical lightcurve of the afterglow of GRB030329, shown with the prediction of the double jet model [11]. (bottom panel) X-ray observations reported by Tiengo et al. [132, 133] with predictions of model 1. Contribution of the narrow jet and the wide jet are shown separately as the dashed and the dotted line respectively. The total flux is shown as the solid curve.

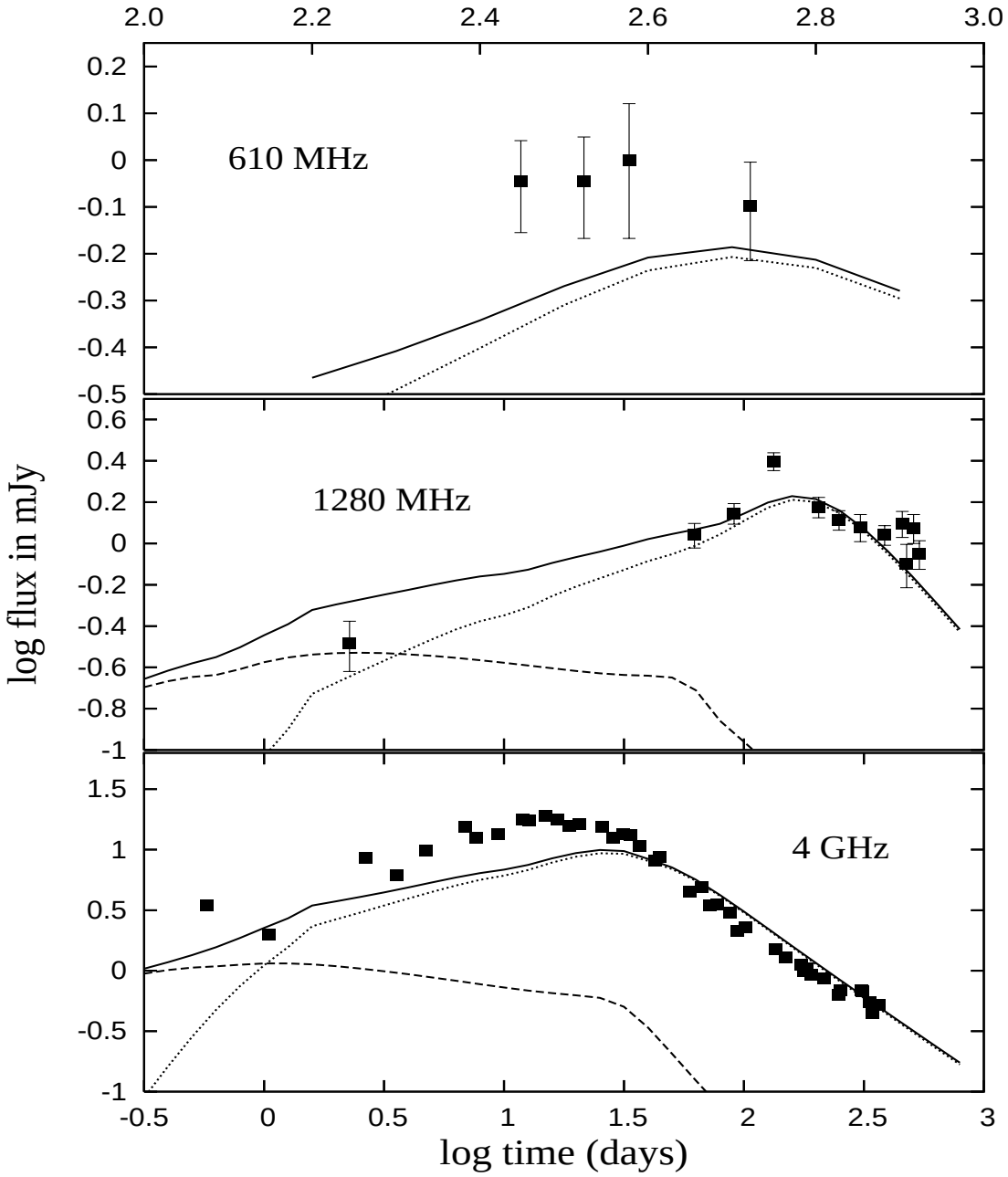

Figure 5.2. Low frequency radio observations along with the predictions of the two jet model. Similar to the previous figure, the narrow jet is represented by dashed line while the wide jet by dotted line. The total flux is shown as a solid curve. The peak of 1280 represent the fireball becoming optically thin in that frequency, as mentioned in the text, the model underpredicts the peak flux, so is the refreshed jet model. Early data of 4 GHz is affected by scintillation.

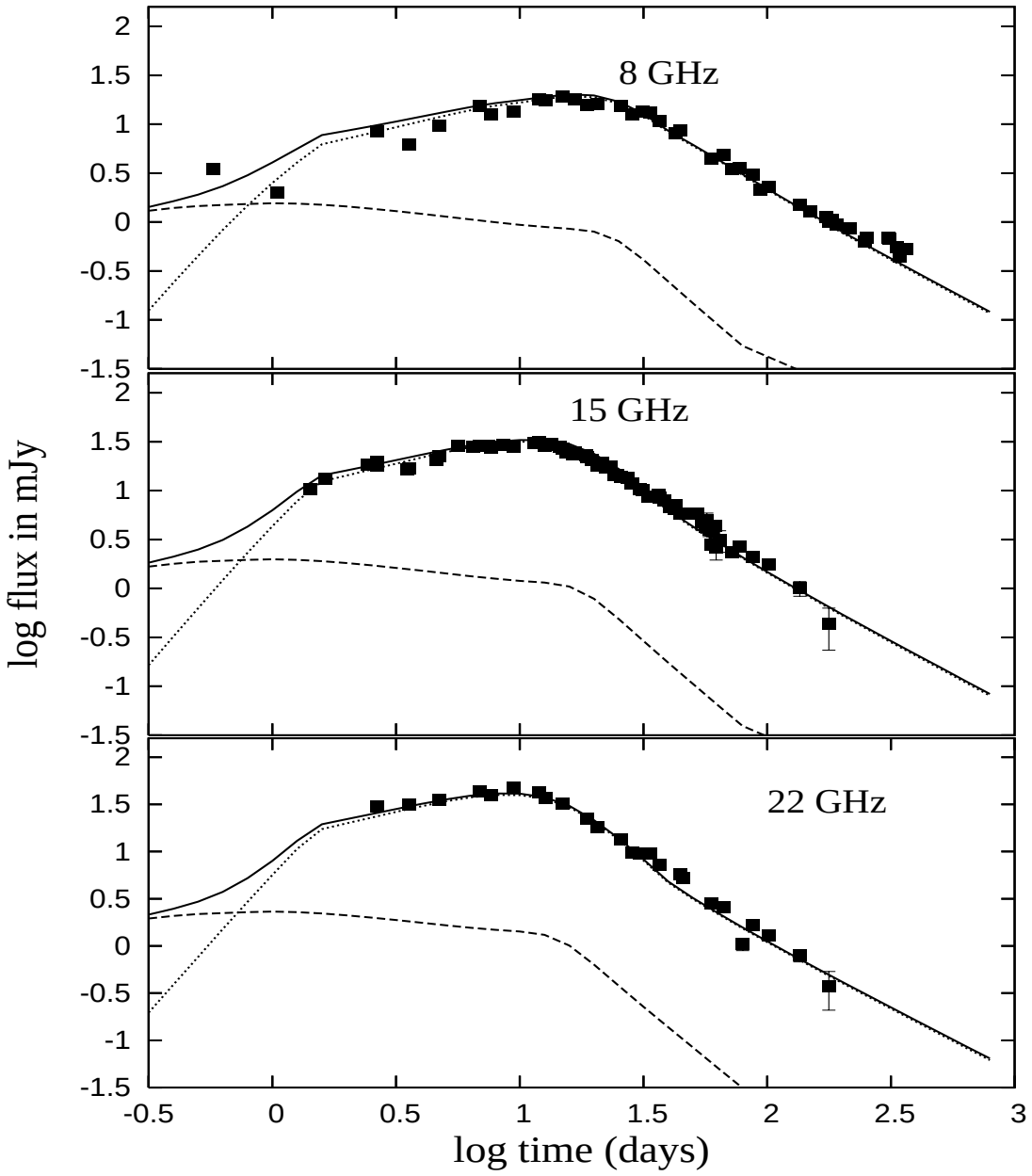

Figure 5.3. The cm observations from VLA along with the model.

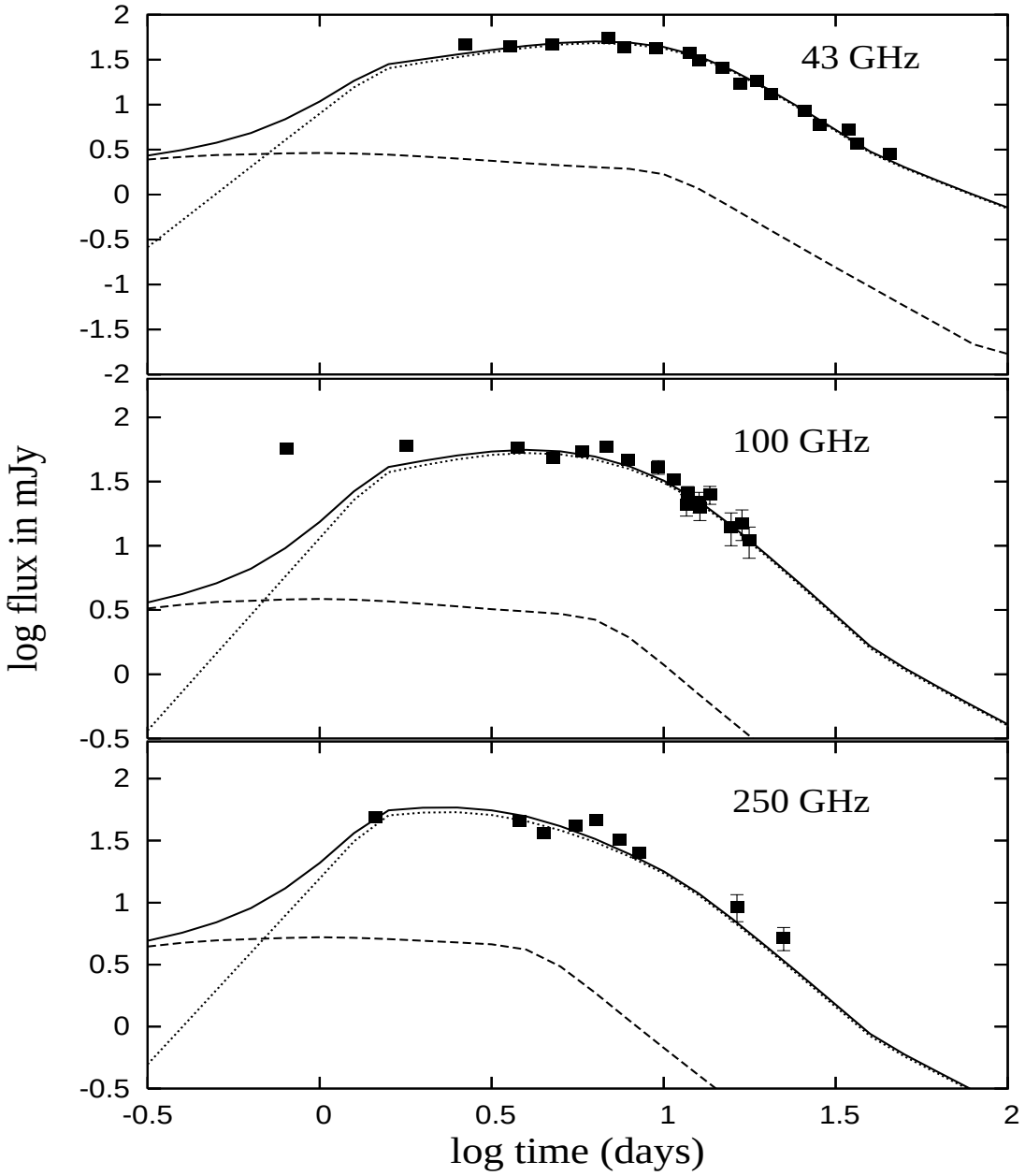

Figure 5.4. High frequency radio observations and model predictions. As noted in the text, the measurements in 100 GHz around 0.8 days is not explained by the model. Even the refreshed jet model fails.

ical parameters of the fireball, namely E, ϵ_e and ϵ_B undergo a change after re-energization, while the ambient density n remains the same. We allow these physical parameters to be determined by the model fits.

Fits to multiwavelength observations with this model (model 2) are shown in figs. 5.5 – 5.8. We excluded the same set of data in these fits as done in model 1. The minimum $\chi^2_{\rm DOF}$ we obtained with this model is 24.5, slightly higher than the value for the previous model. Here again, the χ^2 is dominated by the optical band as well as the low radio frequencies. Both models underpredict the flux at 1280 MHz peak by a factor of 2. But it is difficult to make a distinction between model 1 and model 2 from the small difference in the χ^2. Parameters for the initial, narrow jet are nearly the same as those listed in section 5.2.2 except the self absorption frequency ν_a ($2.9^{+0.8}_{-0.06} \times 10^9$ Hz), which is implied by the value of n inferred from the parameters of the jet after re-energization. Parameters of the refreshed jet are only marginally different from that of the wide jet discussed in section 5.2.1 We obtain a p of 2.24 ± 0.02, t_j of $10^{+2.3}_{-1.0}$ days, and at 9.8 days, a cooling frequency of $5.0^{+2.1}_{-1.5} \times 10^{14}$ Hz, and a marginally reduced self absorption frequency of $1.1^{+0.3}_{-0.05} \times 10^{10}$ Hz. The non-relativistic transition time $t_{\rm nr}$ is $63^{+13.5}_{-30}$ days. The number density of the ambient medium is inferred to be $6.7^{+13.}_{-3.}$. We infer the fractional energy content in relativistic electrons (ϵ_e) and magnetic field (ϵ_B) to be $0.53^{+0.5}_{-0.4}$ and $4^{+2.5}_{-1.3} \times 10^{-4}$ respectively for the initial (narrow) jet, and $0.103^{+0.05}_{-0.01}$ and $1.0^{+1}_{-0.5} \times 10^{-3}$ for the refreshed (wide) jet. We derive an isotropic equivalent energy of $4.6^{+1.6}_{-0.6} \times 10^{52}$ erg for the original jet, which has an initial opening angle of $6.5^{+0.3}_{-0.1}$ degrees. This corresponds to a total energy content of $1.5^{+6}_{-2.8} \times 10^{50}$ ergs in the jet. After re-energization, which is assumed to end around ~ 1.5 days, the total energy content of the jet increases to $1.4^{+5.9}_{-1.7} \times 10^{51}$ erg, and the jet widens to $16.9^{+0.1}_{-0.03}$ degrees.

The transition to the refreshed physical parameters of the jet is expected to be gradual, over the time required to establish a new equilibrium. The timescale for achieving a new Blandford-McKee structure will be roughly equal to the time the second wave requires to cross the existing shocked shell. This time, in the co-moving frame, can be estimated as the thickness of the matter in the co-moving frame of the shock, divided by c, which in the observer's frame will be

$\Delta t \approx R/(a\Gamma_{\rm old}\Gamma_{\rm new}c)$, where $a \sim 5-10$. At 1.5 days, when the new power law phase begins, we calculate the bulk Lorentz factor ($\Gamma_{\rm new}$) to be ~ 2.3, by extrapolating the value of Γ from the jet break time. Extrapolation for the initial jet produces $\Gamma_{\rm old}$ to be close to this value. Hence Δt will be of the order of $0.2-0.3$ days. From a close examination of the optical lightcurve, we find that the refreshment episode could begin at ~ 1.2 days and at ~ 1.5 days, the new power law phase begins.

5.4 Discussion

We have seen above a comparison between the parameters of the two models. We now discuss their compatibility with the constraints imposed by other available observations of the afterglow. The estimated angular size of the fireball [131] can be reproduced by models with isotropic equivalent energy to external density ratio in the range $10^{50}-10^{52}$ erg cm^{-3} [94]. The parameters extracted from both the models fall close to this range.

Polarization measurements of the afterglow are available in optical [61] and in radio [131] bands. In the optical, the degree of polarization decreases shortly after the jet break at ~ 0.5 days and rapid variations in polarization start occurring around 1.5 days, which according to Greiner et al. [61] could be the beginning of a new power law phase. The linear polarization at 8 GHz ($< 0.1\%$) around 8 days is significantly lower than the optical polarization ($\sim 2\%$), which could be due to the fireball being optically thick at this frequency. This polarization behaviour has been thought to support the double jet model [61, 131]; however this is equally applicable to the refreshed jet.

We point out that the first millimeter-wave observation at 86 GHz by the Swedish-ESO Submillimetre Telescope (SEST) at 0.6 days [111] and the 100 GHz observation at 0.8 days [123] are not well fit by this simple model. Nor does the double-jet model succeed in reproducing this well.

5.5 Reverse Shock

It has been pointed out that the deceleration of the wide jet at 1.5 days is expected to be accompanied by a strong radio flash from the reverse shock [104], which is not observed. This concern remains for the refreshed jet model, too. The two models differ in the nature of the medium in which the second shock front decelerates (in model 1, a normal ISM while in model 2, it is the material already shocked by the first shell). The Sedov length in these two cases are also to be evaluated differently, since in model 1, the shell responsible for the wide jet encounters matter all the way from the progenitor star while in model 2, the second wave of energy passes through the region evacuated by the first jet.

We estimated the reverse shock emission expected in either model, assuming that the shock is ultrarelativistic (thick shell case) [79, 118]. For model 1 there are four relevant regions, namely, normal ISM (0), ISM shocked by the wide jet (1), reverse shocked ejecta (2) and the cold second shell (3). Region 1 and region 2 are separated by a contact discontinuity (CD). We followed the formulation of Kobayashi [79] to obtain the flux expected from reverse shock. In model 2, since the reverse shock originates when the second wave of energy decelerates into the already shocked material, the space ahead of the CD will be divided into three regions instead of two [80]. The five relevant regions in this case are: the ISM (0), the ISM shocked by the first wave (1), ISM additionally shocked by the second wave (2), reverse shocked ejecta (3) and the cold second shell (4). A contact discontinuity separates regions 2 and 3. Assuming pressure balance at the CD, and for the ejecta using the assumption that $n_4 R^2$ is constant, (where n_4 is the number density of the cold shell and R is the distance to the CD), one obtains the bulk Lorentz factor (γ_3) and thermodynamic quantities (density and pressure) of region 3. These quantities allow one to estimate the synchrotron emission from that region. The thickness (Δ) of the ejecta is an unknown parameter in both models. For a given Δ the peak flux produced by double jet model is two orders of magnitude lower than the refreshed jet model at the deceleration time of 1.5 days. The computed flux is inversely related to Δ, and the minimum value Δ can reach without overpredicting the flux observed at various bands is $\sim 10^{10}$ cm for model 1, and $\sim 10^{13}$ cm for model 2. More detailed investigations taking into account

detailed hydrodynamics in non-spherical geometry as well as the density structure of a post-jet break fireball may be necessary to get a better estimate.

5.6 SN 2003dh

The optical emission observed at times later than ~ 7 days cannot be fully accounted for by the afterglow models discussed so far. We attribute the excess emission at these late epochs primarily to the associated supernova, SN2003dh. We subtract the afterglow flux predicted by the model and the flux due to the host galaxy [57] from the observed data to estimate the contribution from the supernova. Fig. 5.9 displays the flux attributed to the supernova in the two models discussed above. The K-corrected light curve of SN1998bw [53] appropriate for the redshift of GRB030329 is shown along with the residuals for comparison. While being similar in temporal behaviour, the residuals from model 1 are fainter by ~ 0.3 mag in comparison to an equivalent SN1998bw lightcurve. In case of model 2, this difference is ~ 0.4 mag. These results compare well with the estimate of Lipkin et al. who find that an SN1998bw lightcurve, diminished by 0.3 magnitude, is required to fit the observed data.

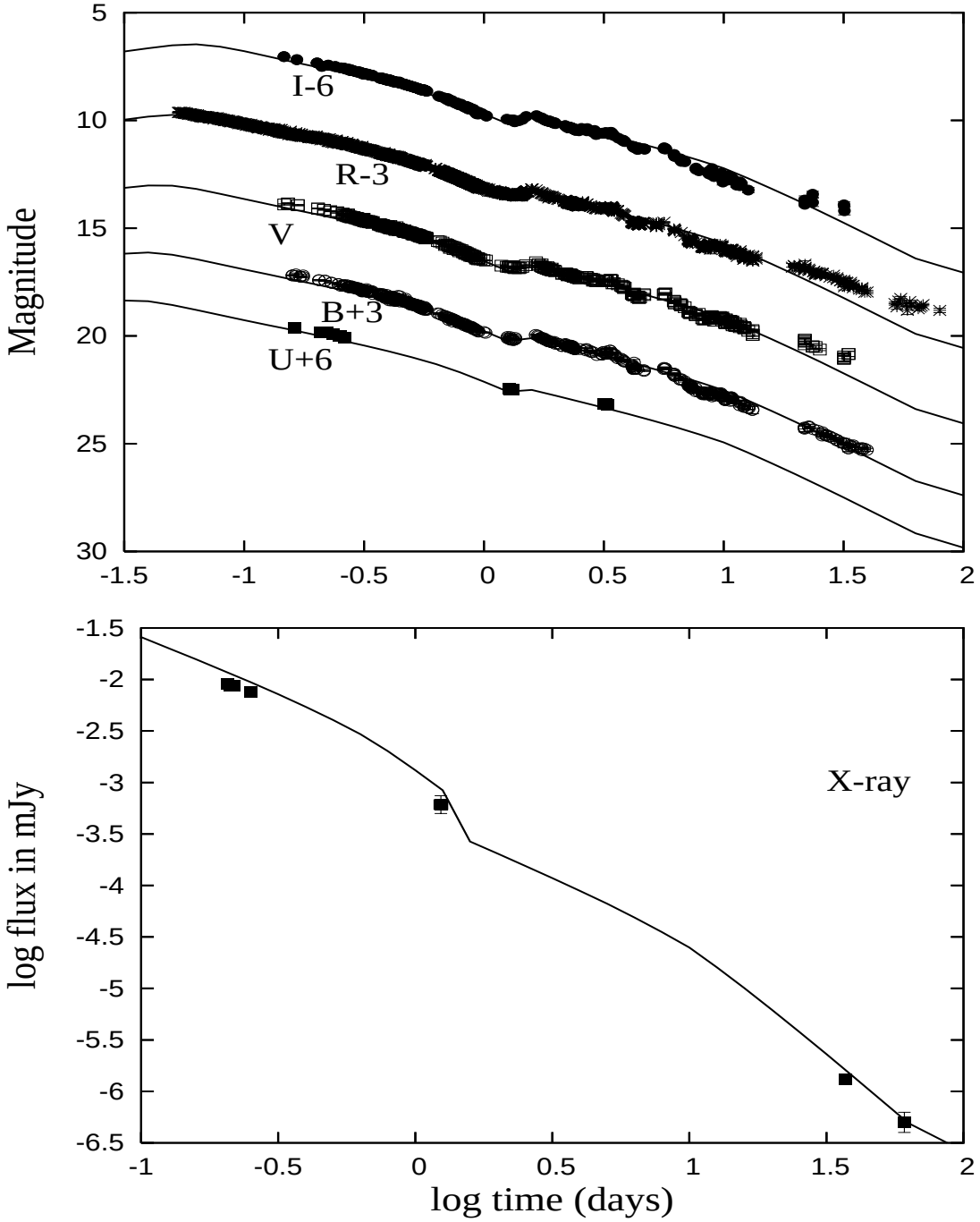

Figure 5.5. (top panel) The Optical lightcurve of the afterglow of GRB030329, along with predictions from model 2, which assumes a transition of an initially narrow jet to a wider jet at ~ 1.5 days. (bottom panel) X-ray observations, with predictions from the model. The flattening seen at late times is due to the transition into non-relativistic regime at ~ 63 days.

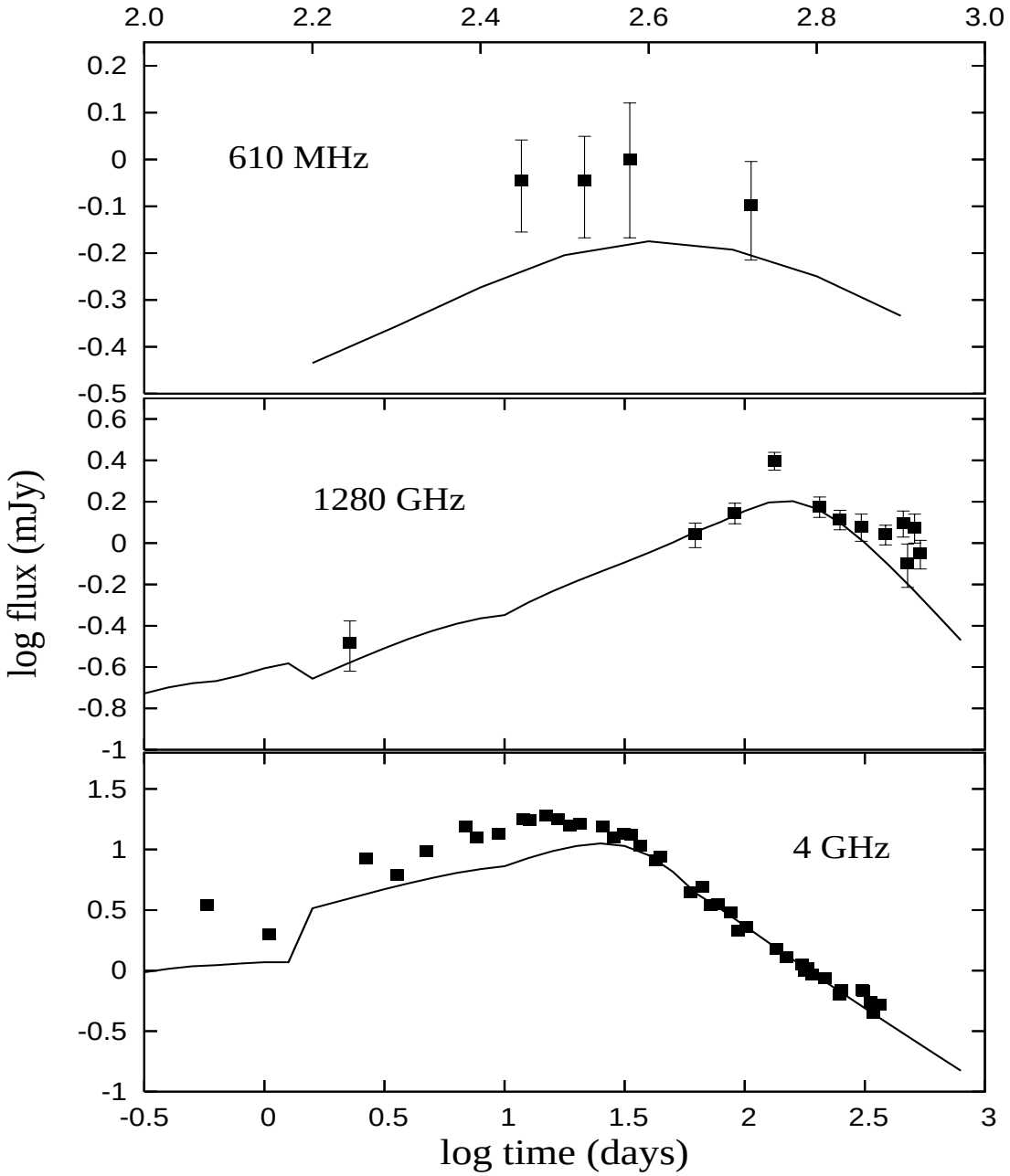

Figure 5.6. Low frequency radio observations. Model 2 also underpredicts the peak flux in 1280 MHz.

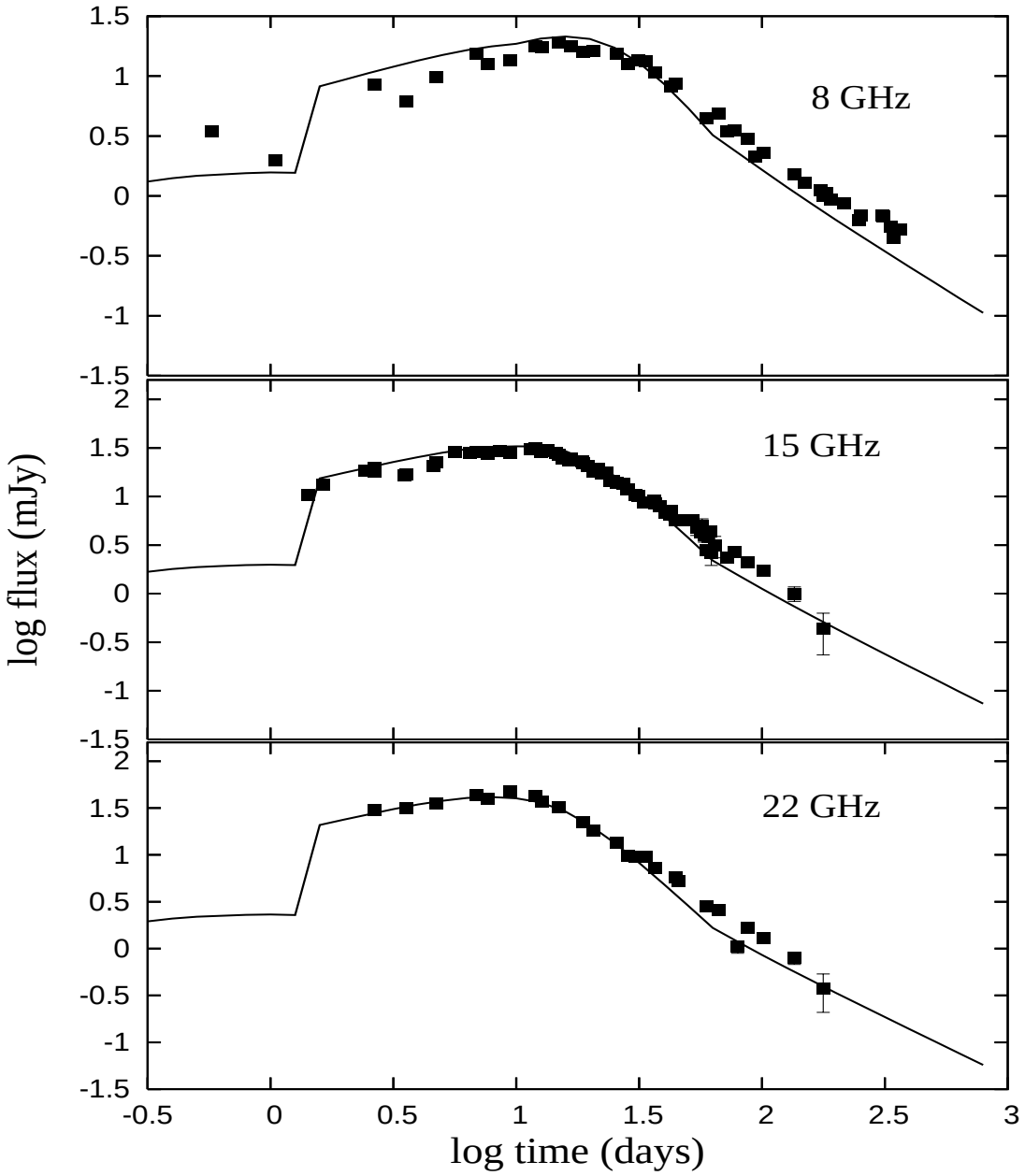

Figure 5.7. The cm observations from VLA along with the predictions of the refreshed jet model.

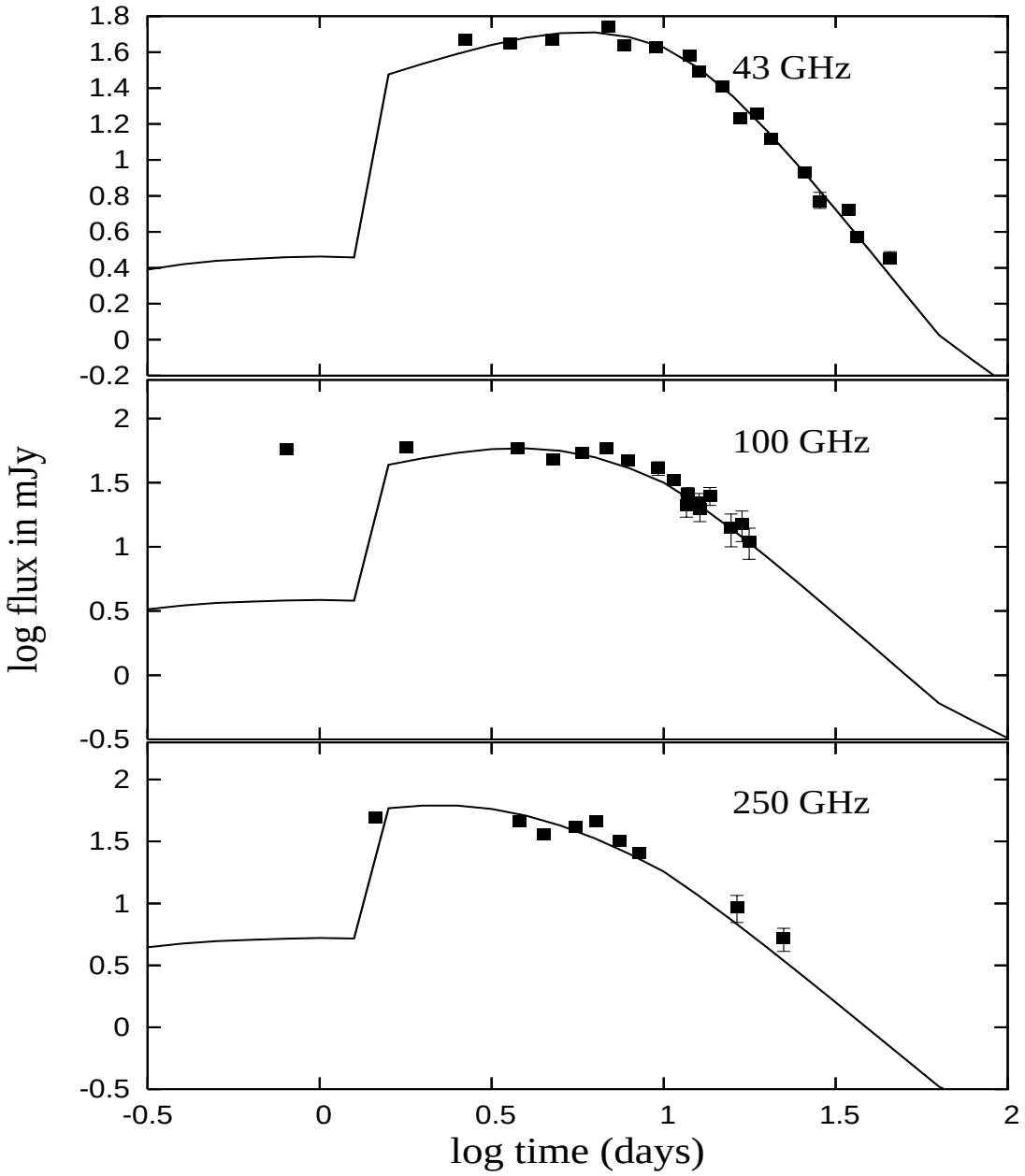

Figure 5.8. High frequency radio observations. The measurements in 100 GHz around 0.8 days is not explained by the model.

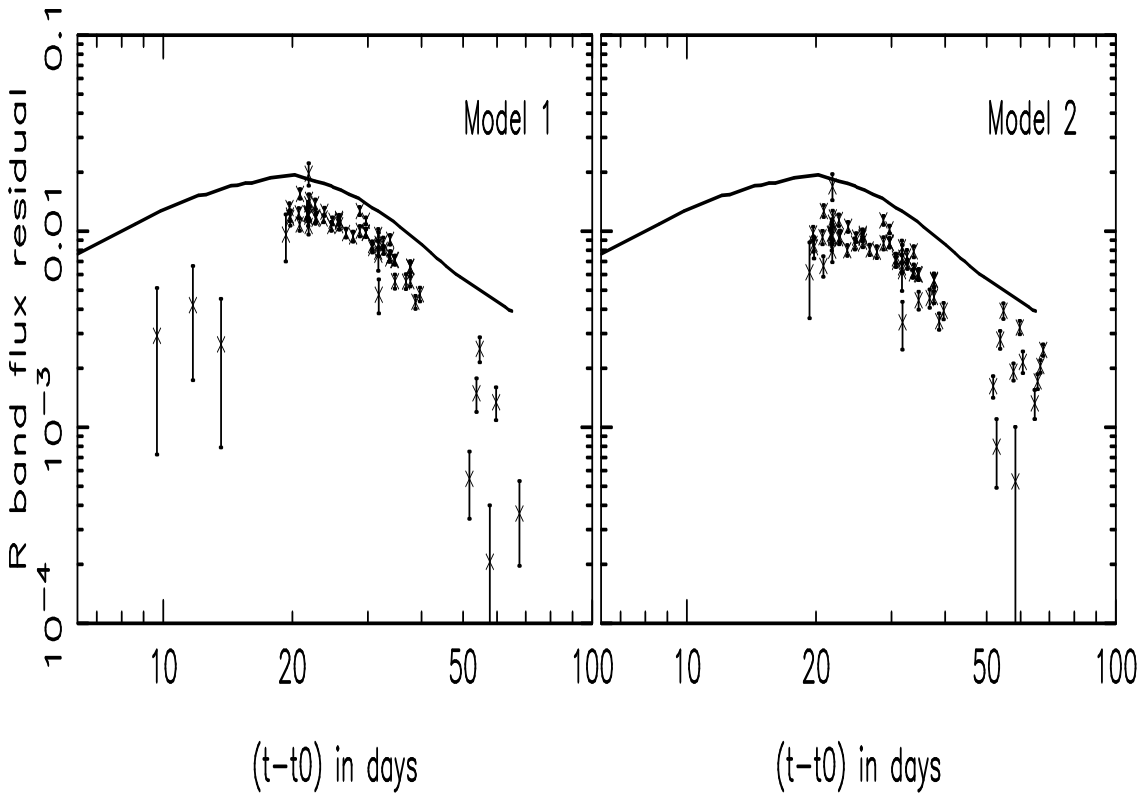

Figure 5.9. R-band residuals for epochs beyond $\sim$ 7 days, after subtracting the modeled flux of the afterglow and the contribution of the host galaxy ($R = 22.6$ [57]) from the observed flux. The two models are shown in adjacent panels. This shows the R-band contribution needed from the associated supernova SN2003dh to explain the total observed light from the OT. The solid line is the red-shifted K-corrected SN1998bw R-band lightcurve, shown for comparison.